

prisms with the SrSi_2 structure has been illustrated by Holden (1971). There is evidence that the SrSi_2 and $\beta\text{-Mn}$ packings serve as the basis of the cubic structures observed in the 'blue phases' of cholesteric liquid crystals (Meiboom, Sammon & Berremann, 1983, and references therein).

I am grateful to the Beevers Miniature Models Unit of the Chemistry Department of Edinburgh University for the ball-and-spoke frameworks used for the models of cylinder packings, which were made by Lita R. O'Keeffe. This work was supported by a grant (DMR 8813524) from the US National Science Foundation.

References

- ANDERSSON, S. & O'KEEFFE, M. (1977). *Nature (London)*, **267**, 605-606.
- FISCHER, W. & KOCH, E. (1983). In *International Tables for Crystallography*, Vol. A, edited by T. HAHN. Dordrecht: Kluwer.
- HOLDEN, A. (1971). *Shapes, Space and Symmetry*. New York: Columbia Univ. Press.
- International Tables for Crystallography* (1983). Vol. A. Dordrecht: Kluwer.
- JANSON, K., SCHÄFER, H. & WEISS, A. (1965). *Angew. Chem.* **77**, 258-259.
- KASPER, J. S. & RICHARDS, S. M. (1964). *Acta Cryst.* **17**, 752-755.
- MEIBOOM, S., SAMMON, M. & BERREMANN, D. W. (1983). *Phys. Rev. A*, **28**, 3553-3560.
- NYMAN, H., CARROLL, C. E. & HYDE, B. G. (1991). *Z. Kristallogr.* **196**, 39-45.
- O'KEEFFE, M. (1991). *Z. Kristallogr.* **196**, 21-37.
- O'KEEFFE, M. & ANDERSSON, S. (1977). *Acta Cryst.* **A33**, 914-923.
- O'KEEFFE, M. & HYDE, B. G. (1980). *Philos. Trans. R. Soc. London*, **295**, 553-623.
- SCHNERING, H. G. VON & NESPER, R. (1987). *Angew. Chem. Int. Ed. Engl.* **26**, 1059-1080.
- SHOEMAKER, C. B., SHOEMAKER, D. P., HOPKINS, T. E. & YINDEPIT, S. (1978). *Acta Cryst.* **B34**, 3573-3576.
- SHUBNIKOV, A. V. & KOPTSIK, V. A. (1974). *Symmetry in Science and Art*. New York: Plenum.
- SMITH, J. V. (1982). *Geometrical and Structural Crystallography*. New York: Wiley.
- VOLTEN, A. (1968). *Constructie in Staal*. Otterloo, Netherlands: Rijksmuseum Kröller-Müller.

Acta Cryst. (1992). **A48**, 884-901

Decagrammal Symmetry of Decagonal $\text{Al}_{78}\text{Mn}_{22}$ Quasicrystal

BY A. JANNER

Institute for Theoretical Physics, University of Nijmegen, Toernooiveld, 6525 ED Nijmegen, The Netherlands

(Received 26 November 1991; accepted 6 May 1992)

Abstract

General ideas about symmetries of quasicrystals based on simple self-similar tiling models and their mathematical formulation in terms of higher-dimensional multimetric space groups find extensive confirmation in the structure of the decagonal $\text{Al}_{78}\text{Mn}_{22}$ quasicrystal phase. There is an incredible richness and variety of symmetries involving, in addition to mirror, rotation, translation and screw-rotation symmetries, planar and linear scalings as well, together with involutions generating those scalings, with and without associated nonprimitive translations. The linear parts of these symmetries generate a point group of infinite order, not yet fully investigated but, up to now, consistent with the symmetry of a self-similar decagram. The applicability of these symmetries to the atomic structure of the quasicrystal $\text{Al}_{78}\text{Mn}_{22}$ observed in nature requires the concept of higher-dimensional crystal forms and their projections in the physical space and in the internal space, respectively.

1. Introduction

One of the most striking characteristics of the diffraction pattern of many quasicrystals is the (discrete) scaling invariance of the positions of the Bragg peaks (Kuriyama & Long, 1986; Long & Kuriyama, 1986; Ostlund & Wright, 1986). That property is also found in simple classical models of quasicrystal structures described in terms of aperiodic tilings. Examples are, in one dimension, the Fibonacci and the octagonal chains and, in two and three dimensions, the Penrose tiling. The scaling property of the diffraction pattern is a consequence of the fact that those tilings are invariant with respect to appropriate inflation/deflation transformations. This means that, by combining inflation (deflation) with a rescaling of the distances, one gets the original pattern back.

The aim of the present paper is to demonstrate that scaling invariance can occur in quasicrystal structures, when described in terms of atomic positions. That will be shown by means of the concrete example of the decagonal $\text{Al}_{78}\text{Mn}_{22}$ quasicrystal phase on

the basis of the structure refinement by Steurer (1991).

Before going into more details, a few important facts have to be kept in mind to avoid misunderstanding. First of all, the intensity of the diffraction pattern is not scaling invariant. It is in the positions of the Bragg peaks that one finds evidence for possible scaling symmetries. Such symmetry is also implicit in the intensity distribution of the diffraction pattern. Secondly, considering the direct space, the charge density of the quasicrystal is also not scaling invariant: an atom having a well defined electron cloud around it is incompatible with dilation (or contraction) symmetry. Scaling only concerns atomic positions, *i.e.* the structure in a point-atom approximation. Thirdly, even a discrete atomic pattern never has a scaling-symmetry group. Indeed, a minimal finite interatomic distance is always involved, so that at most there is a semigroup of invariant scaling transformations. Connected with that, one has to be aware that admitted inflation/deflation transformations of a self-similar tiling or of a scaling-invariant quasicrystal are not automorphisms of the atomic positions defined in the physical space but monomorphisms only. Nevertheless, scaling symmetry represents an essential feature for understanding the structure of $\text{Al}_{78}\text{Mn}_{22}$.

It is well known that lattice-translational symmetry is recovered, for an ideal infinite quasicrystal structure, by means of an embedding in a higher-dimensional space (the superspace). For this embedded structure, the transformations leading to scaling in space do have all the properties required of crystallographic symmetries.

Crystals are never infinite and it is appropriate to make a distinction between possible, occupied and virtual atomic positions, 'occupied' meaning the possible positions inside a given volume (normally a crystal growth form) and 'virtual' the possible positions that are outside that volume. In the case of an embedded quasicrystal this is of fundamental importance for understanding the nature of the basic facts pointed out above. As explained later and discussed in a previous paper (Janner, 1992), a crystal form fixes the volume of the occupied atomic positions in the superspace and gives by projection a corresponding form in the physical space. Another form is obtained from a projection into the internal space (the orthogonal complement). The form in physical space is responsible for a maximum value of the interatomic distances (as in the case of crystal-growth forms), whereas the form in the internal space leads to finite minimal distances and in the limit of an infinite quasicrystal it corresponds to what is usually denoted as an atomic surface (Steinhardt & Ostlund, 1987). It is, however, worth pointing out that these volumes are defined microscopically and involve a set of equivalent atomic positions, whereas a crystal growth

form is a macroscopic object defined for the crystal as a whole.

In both cases, the crystal forms break the space-group symmetry. In normal crystals, the breaking of the symmetry, *e.g.* of lattice translations, only affects atoms whose positions are near the boundaries. One can say the same for embedded quasicrystals but, in physical space, even atoms inside the quasicrystal are near to atomic positions that are at the surface of the internal crystal form, all atoms being affected by the requirement of finite minimal interatomic distances.

There are, therefore, symmetries in the superspace that in the physical space only imply possible structural properties of the quasicrystal. In general, global superspace symmetries are reduced in space to a set of local ones. Furthermore, because of aperiodicity, it is only possible to verify locally whether or not those structural relations are present in a given quasicrystal. Quasiperiodicity ensures, on the other hand, that the same local environment is repeated throughout the structure.

To restrict considerations to a local region is also meaningful from another point of view. Scaling transformations are of infinite order, as are the corresponding superspace symmetry operations. As in the unit cell the number of atomic positions is finite, only special Wyckoff positions of finite multiplicity are allowed. As already mentioned, a continuous charge distribution, perfectly compatible with the rotational point-group elements, represents a symmetry-breaking element for the scaling properties of the quasicrystal. Going beyond a local region by repeating application of an inflation transformation dramatically increases the symmetry-breaking effects and becomes meaningless for structural relations at too large distances.

2. Superspace embedding

Quasicrystals belong to the class of incommensurate crystals, which is characterized by Bragg diffraction peaks with positions generating a \mathbb{Z} -module M^* of dimension 3 and rank n . Owing to incommensurability, n is larger than 3; in the case of the decagonal phase one has $n=5$. As shown by Bak (1985) and Janssen (1986), the superspace approach is applicable to quasicrystals.

By embedding the charge density $\rho(r)$ according to the scheme

$$\rho(r) \xleftrightarrow{\text{FT}_3} \hat{\rho}(h_1, \dots, h_n) \equiv \hat{\rho}_s(h_1, \dots, h_n) \xleftrightarrow{\text{FT}_n} \rho_s(r_s), \quad (1)$$

where FT_n denotes the n -dimensional Fourier transform, one gets a lattice-periodic density $\rho_s(r_s)$ defined in an n -dimensional space (the superspace). The original \mathbb{Z} -module appears as a projection of the

reciprocal lattice Σ^* of ρ_s . For a proper characterization of the conditions for reflections in terms of an n -dimensional space group G (the superspace group), the embedding of M^* onto Σ^* has to be such that the rotational symmetries of the diffraction pattern (and thus of M^*) are mapped into rotational symmetries of ρ_s (and thus of Σ^*). Accordingly, a Euclidean invariant metric is defined in the superspace and by duality a lattice Σ follows, describing the translational symmetry of ρ_s .

The projection of Σ into the physical space yields another \mathbb{Z} -module M , which in the case of quasicrystals has the same rank n as M^* (and also, of course, the same dimension). Both projections are one-to-one mappings. The general situation can be represented schematically by

$$M^* \xleftarrow{\text{projection } \pi^*} \Sigma^* \xleftrightarrow{\text{duality}} \Sigma \xrightarrow{\text{projection } \pi} M. \quad (2)$$

As can be seen, there are two alternative embeddings: a reciprocal-space embedding of M^* onto Σ^* defined as in (1) and a direct-space embedding of M onto Σ presented below. These two embeddings are equivalent, but distinct.

The meaning of M follows from (1) and (2): the relative positions in space of atoms, which in the superspace are translationally equivalent, can be expressed as integral linear combinations of the n basis vectors generating the \mathbb{Z} -module M . The corresponding translationally equivalent atomic positions of a quasicrystal can thus be labeled by a set of n integers (indices), in an analogous way to the labeling of the Bragg reflections in reciprocal space.

The projection into the physical space of all translationally equivalent atoms in the superspace defines the possible positions. These form a dense set. The discrete set of the occupied atomic positions observed in the quasicrystal follows from the possible ones lying inside an appropriate acceptance region in superspace. We call that region a crystal form CF_s (as mentioned above) if its boundaries are equivalent with respect to the site symmetry. Therefore, the region CF_s requires a label $i \in I_G$ indicating which set of translationally equivalent positions is involved. In the superspace one thus has (in the point-atom approximation)

$$\rho_s(r_s) = \sum_{i \in I_G} \sum_{m_1, \dots, m_n} \delta(r_s - m_1 a_{1s} - \dots - m_n a_{ns}) \times CF_S^{(i)}(m_1, \dots, m_n), \quad (3)$$

with the summation over all integers m_k and where a_{1s}, \dots, a_{ns} generate the lattice Σ . Whenever the meaning is clear, we will omit the superscript i . The characteristic function CF_s takes the value 1 for the atomic positions inside the crystal form and 0 for those outside. From CF_s one gets a crystal form CF in the physical space and another, CF_I , in the internal

space, according to

$$CF_s = (CF, CF_I), \quad (4)$$

with $CF = \pi CF_s$ and $CF_I = \pi_I CF_s$. For a given i value, all these forms have the same point-group symmetry since the symmetry rotations involved leave invariant the external and the internal subspaces and generate isomorphic point groups.

Equations (4) and (3) define the direct superspace embedding of a quasicrystal given by

$$\rho(r) = \sum_{i \in I_G} \sum_{m_1, \dots, m_n} \delta(r - m_1 a_1 - \dots - m_n a_n) \times CF^{(i)}(m_1, \dots, m_n), \quad (5)$$

where the basis a_1, \dots, a_n generates the \mathbb{Z} -module M and is the projection of the lattice basis a_{1s}, \dots, a_{ns} . The atoms of the quasicrystal are situated in space within the crystal form CF and have an internal position vector that is inside the crystal form CF_I . In other words, the direct superspace approach corresponds to the cut-projection method (Katz & Duneau, 1986a, b) and, as already pointed out, CF_I corresponds in the reciprocal superspace approach to an atomic surface.

3. Euclidean symmetry

The structural data of the decagonal phase Al₇₈Mn₂₂ are taken from the papers by Steurer (1989, 1991), the reciprocal superspace embedding from Janssen (1986) and from what can be found in the articles by Yamamoto & Ishihara on the relation between decagonal quasicrystals and Penrose patterns (Ishihara & Yamamoto, 1988; Yamamoto & Ishihara, 1988). Here, the analysis of the symmetries will be done in the frame of a direct superspace approach, following the ideas on admissible quasicrystal symmetries based on self-similar tilings (Janner, 1991b).

The \mathbb{Z} -module M^* of the Bragg peaks is generated by

$$a_k^* = a^*(\cos 2\pi k/5, \sin 2\pi k/5, 0), \\ k = 1, \dots, 4 \quad \text{and} \quad a_5^* = c^*(0, 0, 1), \quad (6)$$

where the components are expressed with respect to an orthonormal basis and $a^* = 0.2556$ (1) and $c^* = 0.08065$ (5) \AA^{-1} . The reciprocal lattice Σ^* , such that the three-dimensional rotational symmetries of the diffraction pattern define five-dimensional rotations leaving that lattice invariant, is generated by the basis

$$d_k^* = [a_k^*, c_0 a_{2k}^*], \quad k = 1, \dots, 4 \quad \text{and} \quad d_5^* = [c^*, 0] \quad (7)$$

where the splitting is according to the vector components in the external and internal space, respectively: $x = [x_E, x_I]$. Equation (7) has to be understood in the following way. One starts from a six-dimensional Euclidean space, a direct sum of two three-dimensional spaces for which the vectors

a_k^* , $k = 1, \dots, 5$, are defined as above. Thus the external space is three-dimensional, whereas the internal space, which involves $c_0 a_{2k}^*$ for $k = 1, \dots, 4$ only, is two-dimensional. Therefore, the superspace is five-dimensional and is spanned by the lattice basis d_1^*, \dots, d_5^* . The dual basis generating the direct lattice Σ is given by

$$d_k = (2/5)[a_k, (1/c_0)a_{2k}], \quad k = 1, \dots, 4 \quad \text{and} \quad d_5 = [c, 0], \quad (8)$$

where $a_k = a[\cos(2\pi k/5) - 1, \sin(2\pi k/5), 0]$, $a_5 = c(0, 0, 1)$ and $aa^* = cc^* = 1$. In the following, $c_0 = 1$ is chosen, which is justified when representing scaling symmetries in space in terms of hyperbolic rotations in superspace, as explained below.

The Euclidean holohedry of the lattice Σ is the point group $K_e = 10/mmm$ generated by:

$$R_1(a) = R_1(d) = \begin{pmatrix} 0 & 0 & -1 & 0 & 0 \\ 0 & 0 & 0 & -1 & 0 \\ 1 & 1 & 1 & 1 & 0 \\ -1 & 0 & 0 & 0 & 0 \\ 0 & 0 & 0 & 0 & 1 \end{pmatrix} = R = 10; \quad (9)$$

$$R_2(a) = R_2(d) = \begin{pmatrix} 0 & 0 & 0 & 1 & 0 \\ 0 & 0 & 1 & 0 & 0 \\ 0 & 1 & 0 & 0 & 0 \\ 1 & 0 & 0 & 0 & 0 \\ 0 & 0 & 0 & 0 & 1 \end{pmatrix} = m_1; \quad (10)$$

$$R_3(a) = R_3(d) = Rm_1 = m_2 \text{ so that } m_2 m_1 = R; \quad (11)$$

$$R_4(a) = R_4(d) = \begin{pmatrix} 1 & 0 & 0 & 0 & 0 \\ 0 & 1 & 0 & 0 & 0 \\ 0 & 0 & 1 & 0 & 0 \\ 0 & 0 & 0 & 1 & 0 \\ 0 & 0 & 0 & 0 & -1 \end{pmatrix} = m_z. \quad (12)$$

$R(a)$ indicates that the matrix is expressed with respect to the basis a_1, \dots, a_5 of the \mathbb{Z} -module M and $R(d)$ implies that the same matrix is now referred to the lattice basis d_1, \dots, d_5 of Σ . Therefore, $R(a)$ is a three-dimensional rotation, whereas $R(d)$ is a five-dimensional one (Janssen, 1986, 1988). So, in particular, $m_1 = R_2(a)$ is a mirror transformation in three dimensions (m_y according to the orthonormal basis adopted) but in five dimensions $m_1 = R_2(d)$ is an involution and not a mirror as one can see looking at its determinant (+1) and at the eigenvalues (1, 1, 1, -1, -1).

The superspace group of the embedded quasicrystal structure is $G_e = P10_5/mmc$, as determined by Steurer (1989, 1991), justifying the name of the phase. This five-dimensional space group is generated by the

Table 1. *Equivalent positions of $G_e = P10_5/mmc$ occupied in $Al_{78}Mn_{22}$*

Atom 3 is at position (a'), atom 4 at (b'), atom 1 at (c') with $z = 0.1858$ and atom 2 is also at (c') with $z = 0.027$.

| Multiplicity, Wyckoff letter, site symmetry | Coordinates |
|---|--|
| 2, (a'), $\bar{10}m2$ | 0, 0, 0, 0, 0, 0, 0, 0, 0, $\frac{1}{2}$ |
| 2, (b'), $\bar{10}m2$ | $\frac{2}{5}, \frac{2}{5}, \frac{2}{5}, \frac{2}{5}, 0, \frac{3}{5}, \frac{3}{5}, \frac{3}{5}, \frac{3}{5}, \frac{1}{2}$ |
| 4, (c'), $5m$ | $\frac{1}{5}, \frac{1}{5}, \frac{1}{5}, \frac{1}{5}, z, \frac{1}{5}, \frac{1}{5}, \frac{1}{5}, \frac{1}{5}, z, \frac{4}{5}, \frac{4}{5}, \frac{4}{5}, \frac{4}{5}, z + \frac{1}{2}, \frac{4}{5}, \frac{4}{5}, \frac{4}{5}, \frac{4}{5}, \bar{z} + \frac{1}{2}$ |

lattice translations $\Sigma = \{d_1, \dots, d_5\}$ and by:

$$g_1 = \{R|0, 0, 0, 0, \frac{1}{2}\} = 10_5; \quad (13)$$

$$g_2 = \{m_1|0, 0, 0, 0, 0\} = m_1; \quad (14)$$

$$g_3 = \{m_2|0, 0, 0, 0, \frac{1}{2}\} = c; \quad (15)$$

$$g_4 = \{m_z|0, 0, 0, 0, 0\} = m_z. \quad (16)$$

The atoms observed are at the superspace atomic-unit-cell positions $(p/5, p/5, p/5, p/5, z)$, with integer values for p . Four inequivalent atomic positions are occupied. According to Steurer (1991), atom 1 is at $p = 1$ and $z = 0.0642$, atom 2 is at $p = 3$ and $z = 0.123$, atom 3 is at $p = 0$ and $z = 0.25$ and atom 4 is at $p = 2$ and $z = 0.25$. All these atoms have an atomic surface with pentagonal symmetry $5m$, which is the site symmetry in the decagonal plane of these positions.

For our purposes, it is convenient to have the mirror plane at the origin, and that implies a shift by $-\frac{1}{4}$ in the z coordinates determined by Steurer (1991). The equivalent positions of the superspace group $P10_5/mmc$ occupied in the ideal five-dimensional $Al_{78}Mn_{22}$ structure are indicated in Table 1, where \bar{z} stands for $-z$. The Wyckoff letters have been primed because their characterization is a provisional one not based on a complete description.

On the basis of this structural information, one can compute the possible positions of the various equivalent atomic sets and compare these results with the experimental Fourier synthesis. In general, the agreement is amazingly good, despite a certain amount of disorder present in the Al/Mn distribution and the deviations from an ideal planar layer structure visible in the sections parallel to the tenfold axis (See Fig. 5 of Steurer, 1991).

Here, only the data concerning atom 1 are presented and discussed for the layer at $z = 0.1858$, because the properties of the remaining structure are essentially the same and do not give any further insight, as far as the present paper is concerned.

In Fig. 1, the observed and the calculated positions in a decagonal layer perpendicular to the tenfold axis are shown, together with the indices of the occupied positions for atom 1. These indices are the components of the corresponding vectors of the \mathbb{Z} -module

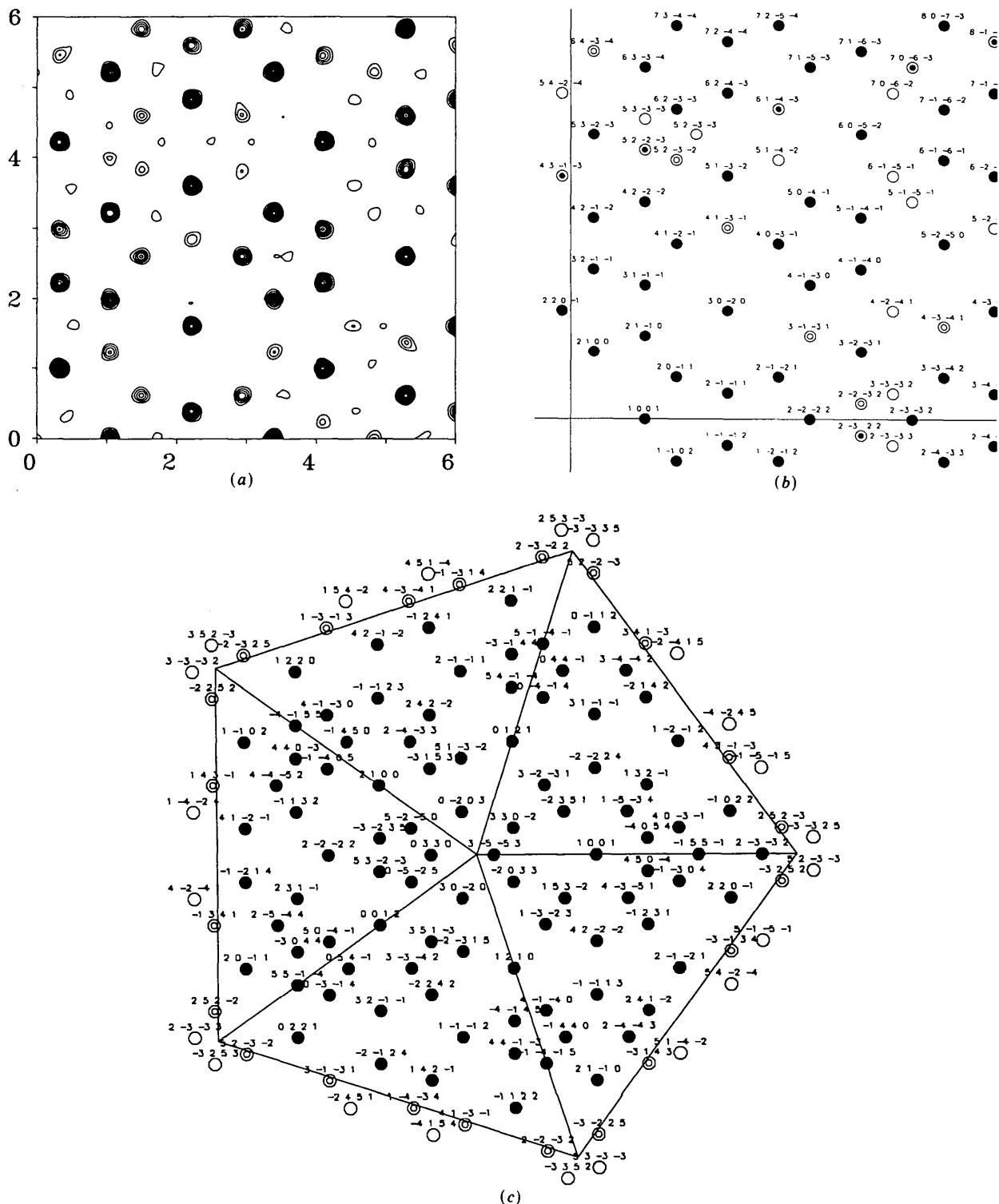


Fig. 1. The charge density distribution in a $25 \times 25 \text{ \AA}$ region of a decagonal plane at $z = 0.1858$ ($x_3 = 0.064$) of the quasicrystal $\text{Al}_{78}\text{Mn}_{22}$. (a) Fourier synthesis according to W. Steurer, who provided this figure. See also Fig. 7(a) of Steurer (1991). (b) Calculated atomic positions in the same decagonal layer as in (a) for increasing size parameter λ_1 of the crystal form $\text{CF}_I^{(1)}$: 0.95 (filled black circles), 1.0 (encircled bullets), 1.05 (double circles) and 1.10 (open circles). The Z-module indices ($z_1 z_2 z_3 z_4$) fixing the positions in space occupied by atom 1 at $r = r_0 + \sum_{k=1}^4 z_k a_k$ are also indicated. Compare with the Fourier density map (a). (c) The occupied positions indexed as in (b) are shown in their internal space arrangement. The pentagonal crystal form $\text{CF}_I^{(1)}$ indicated corresponds to the value $\lambda_1 = 0.95$.

M expressed with respect to the basis a_1, \dots, a_4 , omitting the fifth coordinate, which is constant for a given decagonal plane. The occupation depends on the internal crystal form CF_I , which here has been taken normalized to 0.95, 1.0, 1.05 and 1.10, respectively. The values considered above are approximately τ^2 times larger than the value of 0.403 for λ_1 indicated by Steurer (1991), where $\tau = \frac{1}{2}(1 + 5^{1/2})$ denotes the golden number. In terms of the radial atomic-size parameter λ , the internal crystal form CF_I is the projection into the internal space of a suitably chosen unit cell Ω_0 multiplied by λ . Thus, in particular, one has $CF_I^{(1)} = \lambda_1 \pi_I \Omega_0$. In Fig. 1(c) the distribution of the corresponding internal positions, labeled by their indices, is also shown with respect to the internal crystal form $CF_I^{(1)}$ for $\lambda_1 = 1.0$, showing that indeed additional points (indicated by open circles) are external to that form even if inside $CF_I^{(1)}$. The few discrepancies between internal and external occupied positions are due to truncation effects of the calculations. The size of the external space pattern shown is about $25 \times 25 \text{ \AA}$, to allow a direct comparison with the experimental results already published [Fig. 7(a) of Steurer (1991)]. In Fig. 1 and in the corresponding following figures, the x axis is the abscissa and the y axis is the ordinate.

In Fig. 2, a larger region of about $40 \times 40 \text{ \AA}$ is shown, corresponding to Fig. 8 of Steurer (1991) but now for a single value $\lambda_1 = 1.1$. In Fig. 3, the region shown has been centered around a fivefold axis so that the point symmetry of the pattern is clear. All these plots have been made following the conventions adopted by Janssen (1986) and involve, for the present case ($p = 1$), a shift of the origin by $f = (\frac{4}{5} \frac{4}{5} \frac{4}{5})$. If one wants to check algebraically the validity of the superspace symmetry (limited to those elements leaving the decagonal plane invariant), one has to transform the symmetry elements accordingly: $\{\alpha|a\} \xrightarrow{f} \{\alpha|a + (1 - \alpha)f\}$. For example, for the fivefold rotational point symmetry $\alpha = R^2$ and $a = 0$, one finds $(1 - R^2)f = (4000)$, so that the position (2100) transformed by R^2 becomes the position (1210). Note that, as implied by the Euclidean embedding (8), the corresponding rotation in the internal space is by an angle $4\pi/5$ as one can see in Fig. 1(c).

The other generator of the planar point subgroup is the mirror m_1 of (10), for which $(1 - \alpha)f = 0$; it simply inverts the order of the four indices,

$$m_1(z_1 z_2 z_3 z_4) = (z_4 z_3 z_2 z_1). \quad (17)$$

One can verify this symmetry in both the external and internal spaces. Thus, $5m$ is the point symmetry of the occupied positions of the layer and not only of the possible ones of the ideal superspace crystal: this is so because the crystal forms also have this same point symmetry. Deviation from this symmetry found in the plots is due to truncation effects in the

range of indices adopted for practical reasons in the computation.

The translational invariance with respect to the Z -module M is broken for points outside the crystal form. The validity of this symmetry for the points inside the form is verified by the existence of a

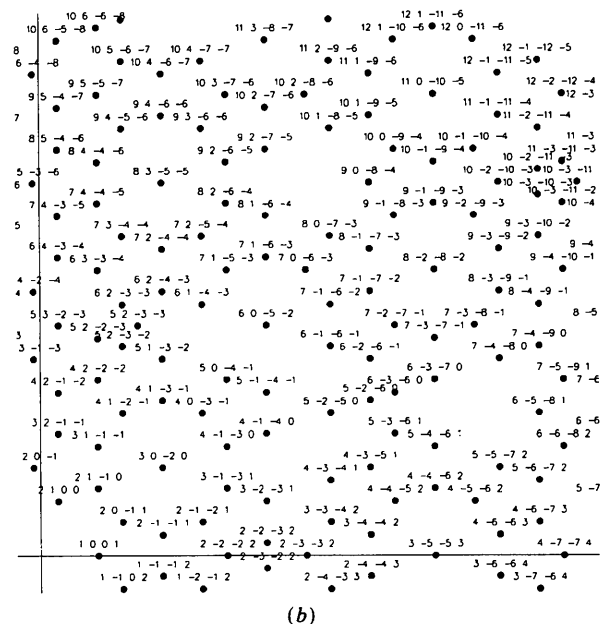
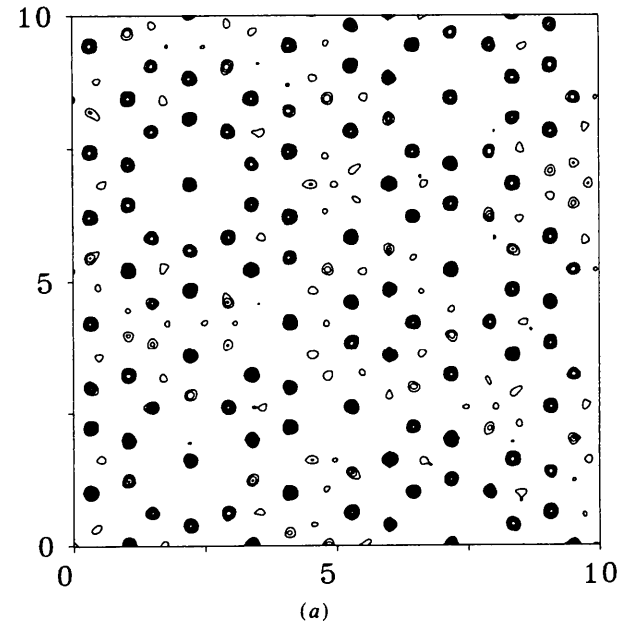


Fig. 2. (a) A $40 \times 40 \text{ \AA}$ region of the same decagonal plane as in Fig. 1(a). Region obtained by W. Steurer from a five-dimensional Fourier synthesis. See Fig. 8(a) of Steurer (1991). (b) The calculated atom 1 positions (for $\lambda_1 = 1.1$) for the same region as in (a), together with the corresponding indices.

consistent indexing of the experimentally observed atomic positions (for translationally equivalent atoms, of course) in agreement with the results of the computation.

In the same way as an ideal crystal arises from a finite crystal by making it invariant with respect to lattice translations and thus infinite, one obtains an ideal quasicrystal from a finite and discrete quasicrystal by adding to the occupied atomic positions the corresponding virtual ones, so that it becomes M -translational invariant and accordingly infinite and dense. The three-dimensional Euclidean symmetry of such an ideal quasicrystal is isomorphic to an n -dimensional space group. In the present case, $P10_5/mmc$ represents at the same time a group of three-dimensional Euclidean transformations and a five-dimensional space group, depending on which set of basis vectors the corresponding group of matrices is referred to. This can be seen as an expression of the crystallographic nature of a quasicrystal. We have adopted here the same Hermann-Mauguin symbol as in the paper by Steurer (1991). The present analysis justifies, in some sense, the use of a nomenclature developed for the three-dimensional crystallographic case. This does not imply that it can be done without inconsistencies in all \mathbb{Z} -module cases. The provisional character of the notation used will be even more apparent in the next sections; this is for obvious reasons.

4. Pseudo-Euclidean symmetry (Minkowskian)

4.1. Scaling

According to Steurer & Mayer (1989) the Bragg peaks are at scaling-invariant positions. Indeed, they write: 'There is no way of uniquely indexing the diffraction pattern of the decagonal reciprocal-lattice planes by multiples of $\tau = (1 + 5^{1/2})/2$ '.

This statement suggests the presence of a scaling symmetry. Indeed, as already indicated in a previous publication (Janner & Janssen, 1990), the decagonal \mathbb{Z} -module M and the corresponding reciprocal module M^* are invariant with respect to a scaling transformation S_{10} with eigenvalues $1, \pm\tau$ and $\pm 1/\tau$. When referred to the basis a_1, \dots, a_5 or to the lattice basis d_1, \dots, d_5 , one finds for S_{10} the matrix

$$S_{10} = \begin{pmatrix} 0 & 0 & \bar{1} & \bar{1} & 0 \\ 1 & 1 & 1 & 0 & 0 \\ 0 & 1 & 1 & 1 & 0 \\ \bar{1} & \bar{1} & 0 & 0 & 0 \\ 0 & 0 & 0 & 0 & 1 \end{pmatrix}. \quad (18)$$

Applying the transformation S_{10} to the atomic positions $p/5, p/5, p/5, p/5, z$ of the ideal embedded $\text{Al}_{78}\text{Mn}_{22}$ structure one obtains, modulo lattice translations, the cyclic permutation (1 3 4 2) of equivalent

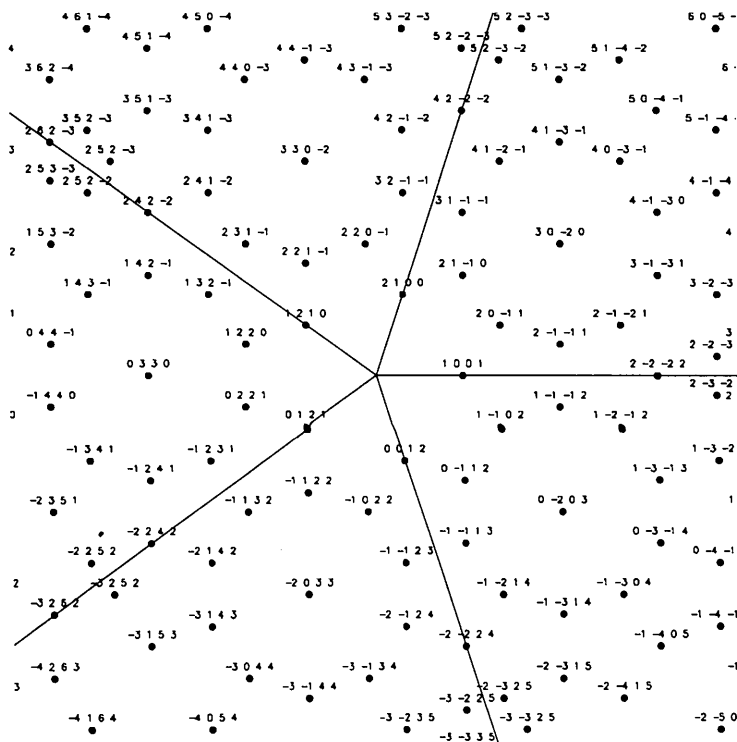


Fig. 3. Coordinates of the occupied positions of atom 1 within a decagonal plane as in Figs. 1 and 2, centered on the fivefold symmetry axis.

positions

$$\begin{aligned} \frac{1}{5}, \frac{1}{5}, \frac{1}{5}, \frac{1}{5}, z &\rightarrow \frac{3}{5}, \frac{3}{5}, \frac{3}{5}, \frac{3}{5}, z \rightarrow \frac{4}{5}, \frac{4}{5}, \frac{4}{5}, \frac{4}{5}, z \\ &\rightarrow \frac{2}{5}, \frac{2}{5}, \frac{2}{5}, \frac{2}{5}, z \rightarrow \frac{1}{5}, \frac{1}{5}, \frac{1}{5}, \frac{1}{5}, z, \end{aligned} \quad (19)$$

which is incompatible with the set of occupied positions indicated in Table 1. Nevertheless, a scaling by a factor τ is structurally relevant for this decagonal phase. The explanation of this apparent paradox will be given below.

The square of S_{10} transforms the occupied positions, modulo lattice translations, in exactly the same way as the rotation R of (9). This is an empirical verification of the compatibility between Euclidean and non-Euclidean crystallographic symmetries, on which new concepts like scale/space group and multi-metrical group are based (Janner, 1990, 1991*b, c*; Janner & Janssen, 1990). Therefore, with $S = S_{10}^2$, the embedded structure is invariant with respect to

$$g_5 = \{S|0, 0, 0, 0, \frac{1}{2}\} = S_{1/2} \quad (20)$$

with

$$S(a) = S(d) = \begin{pmatrix} 1 & 0 & -1 & -1 & 0 \\ 1 & 2 & 1 & 0 & 0 \\ 0 & 1 & 2 & 1 & 0 \\ -1 & -1 & 0 & 1 & 0 \\ 0 & 0 & 0 & 0 & 1 \end{pmatrix} = S = \hat{3}. \quad (21)$$

In the superspace S is a hyperbolic rotation by an angle $\chi = \cosh^{-1}(3/2)$, i.e. $2 \cosh \chi = 3$, which is the value of the trace of the corresponding two-dimensional transformations and this explains the notation $\hat{3}$. In the decagonal plane it gives rise to a dilation by τ^2 and in the internal space there is a contraction by a factor $1/\tau^2$. Indeed, expressing $S(d)$ with respect to the basis D_1, \dots, D_5 given by

$$D_1 = d_1 + d_4, D_2 = d_2 + d_3, D_3 = d_1 - d_4, D_4 = d_2 - d_3, \quad (22)$$

one obtains the direct sum of two two-dimensional hyperbolic rotations

$$S(D) = \begin{pmatrix} 0 & -1 & 0 & 0 & 0 \\ 1 & 3 & 0 & 0 & 0 \\ 0 & 0 & 2 & 1 & 0 \\ 0 & 0 & 1 & 1 & 0 \\ 0 & 0 & 0 & 0 & 1 \end{pmatrix} = \hat{3}. \quad (23)$$

The D basis corresponds to the choice of a nonprimitive $D(1, 3)(2, 4)$ -centered conventional unit cell for Σ . In fact, in an earlier paper (Janner & Ascher, 1969) this was discussed as a basis of a natural lattice.

The positions $(p/5, p/5, p/5, p/5, z)$ are invariant with respect to the translations of the lattice spanned by D_1 and D_2 and lie along the diagonal of the corresponding unit cell. As one sees from the reduced

form (23), S leaves invariant the two planes (D_1, D_2) and (D_3, D_4) . It is a discrete hyperbolic rotation that permutes, according to (19), the pairs of positions $p = 1, p = 4$ and $p = 2, p = 3$, as shown in Fig. 4. In

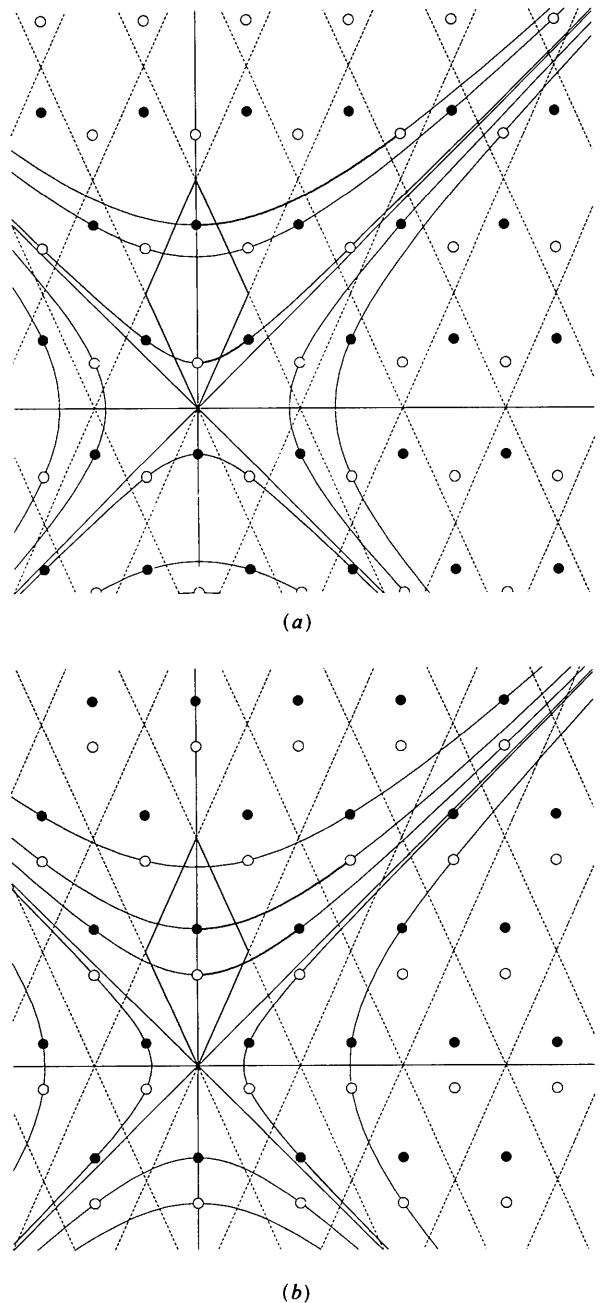


Fig. 4. Scaling-invariant two-dimensional sublattice A_1 of the decagonal five-dimensional lattice Σ . The atomic positions at $(p/5)(D_1 + D_2)$ are indicated in (a) for $p = 4 \pmod 5$ (filled circles) and $p = 1 \pmod 5$ (open circles) and in (b) for $p = 3 \pmod 5$ (filled circles) and $p = 2 \pmod 5$ (open circles). The scaling transformation appears in this subspace as a crystallographic hyperbolic rotation that leaves the lattice invariant and permutes the $p = 1$ and $p = 4$ or $p = 2$ and $p = 3$ positions, respectively. Examples in (a) and (b) are indicated by bold lines.

the five-dimensional space this is the result of the screw hyperbolic rotation g_5 given in (20).

4.2. Local Fibonacci chains

The transformation S_{10} of (18), expressed with respect to the D basis takes the form

$$S_{10}(D) = \begin{pmatrix} \bar{1} & \bar{1} & 0 & 0 & 0 \\ 1 & 2 & 0 & 0 & 0 \\ 0 & 0 & 1 & 1 & 0 \\ 0 & 0 & 1 & 0 & 0 \\ 0 & 0 & 0 & 0 & 1 \end{pmatrix} \sim N_1 \oplus N_1 \oplus 1. \quad (24)$$

From a geometrical point of view, S_{10} represents the direct sum of two two-dimensional N_1 transformations, where N_1 is a hyperbolic rotation by an angle $\varphi = \sinh^{-1} \frac{1}{2}$ combined with a reflection with respect to the asymptotes

$$N_1 = \begin{pmatrix} \cosh \varphi & \sinh \varphi \\ \sinh \varphi & \cosh \varphi \end{pmatrix} \begin{pmatrix} 0 & 1 \\ 1 & 0 \end{pmatrix} = \begin{pmatrix} \sinh \varphi & \cosh \varphi \\ \cosh \varphi & \sinh \varphi \end{pmatrix}, \quad (25)$$

whose square has the form required by S . The transformation N_1 has already been considered in previous papers (see, for example, Janner, 1991c); it was shown to be the superspace embedding of the Fibonacci scaling transformation having eigenvalues τ and $-1/\tau$. One may verify that the sublattice Λ_2 spanned by D_3, D_4 is a square lattice such that D_3 forms an angle α with the asymptote at 45° , where $\tan \alpha = 1/\tau$. As is well known, by orthogonal projection on the line of the lattice points within a strip, one generates a Fibonacci chain (as represented in Fig. 5), which is self-similar with respect to an inflation by τ . The same can be said for the lattice Λ_1 generated by D_1 and D_2 . Indeed, the two lattices are related by Euclidization [see Janner (1991b) for more details], *i.e.* through a hyperbolic rotation by an angle β such that $\tanh \beta = -\tau^{-3} = 2 - 5^{1/2}$ (Fig. 6). The projection considered above is simply the projection π on the physical space.

The p positions that are interchanged by the S_{10} transformation within the (D_1, D_2) plane according to the cyclic permutation (1342) all share the same sublattice Λ_2 . Therefore, as S_{10} leaves this sublattice invariant, even if it interchanges the various p values, it induces a scaling symmetry transformation by τ on the atomic positions lying on the line, which is the π projection of the (D_3, D_4) plane. *Mutatis mutandis*, the situation is the same when considering the internal space instead of the external physical one. In particular, under favorable conditions, the occupied atomic positions on such a line belong to a Fibonacci chain, with missing (virtual) atoms being the result of some mismatch between the required strip region

and the actual (D_3, D_4) -planar intersection of the corresponding crystal form.

All this can be verified for $p = 1$ (atom 1) taking, for example, the atomic position at $P = (1001)$ as the

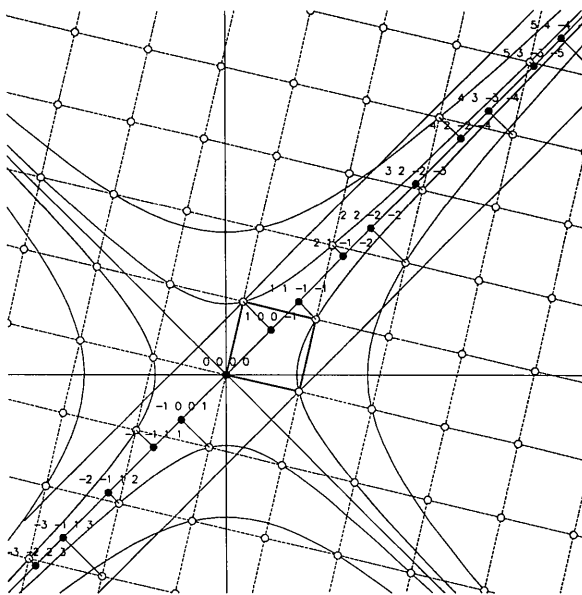


Fig. 5. Another scaling-invariant sublattice Λ_2 spanned by the orthonormal basis D_3 and D_4 . The occupied positions in space, together with the corresponding indices, are given as filled circles. This information will be used in Fig. 7 for illustrating the concept of Fibonacci line.

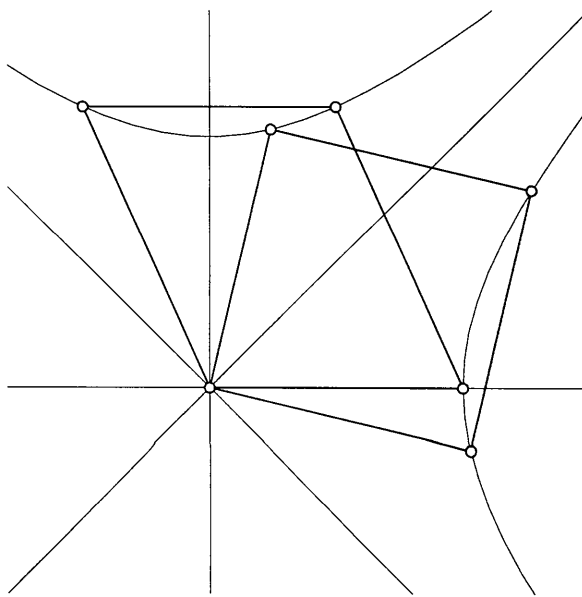


Fig. 6. The two scaling-invariant sublattices Λ_1 and Λ_2 shown in Figs. 4 and 5 are equivalent when considered in an indefinite metric plane. Indeed, they are transformed into one another by the hyperbolic rotation by an angle $\beta = -\tanh^{-1}(5^{1/2} - 2)$. It illustrates the application to an existing quasicrystal structure of the concept of Euclidization introduced in a previous paper.

origin. From Fig. 5, if one adds (1001) to the indices one obtains the Fibonacci chain sequence

$$\begin{aligned} & \dots, (\bar{2}\bar{2}24), (\bar{2}\bar{1}14), (\bar{1}\bar{1}13), (0\bar{1}12), (0002), \\ & (1001), (2000), (21\bar{1}0), (31\bar{1}\bar{1}), (32\bar{2}\bar{1}), (42\bar{2}\bar{2}), \\ & (52\bar{2}\bar{3}), (53\bar{3}\bar{3}), (63\bar{3}\bar{4}), (64\bar{4}\bar{4}), \dots \end{aligned} \quad (26)$$

The occupied positions occurring within a decagonal plane (compare with Fig. 1) and situated along what we shall call a Fibonacci line (as indicated in Fig. 7a) are

$$\begin{aligned} & \dots, (\bar{2}\bar{2}24), (\bar{1}\bar{1}13), (0\bar{1}12), (1001), (21\bar{1}0), \\ & (31\bar{1}\bar{1}), (42\bar{2}\bar{2}), (52\bar{2}\bar{3}), (53\bar{3}\bar{3}), (63\bar{3}\bar{4}), \dots \end{aligned} \quad (27)$$

whereas the missing ones are the corresponding virtual positions. Fig. 7(b) shows that these virtual positions, aligned with respect to the occupied ones, are indeed external with respect to the internal crystal form $CF_1^{(1)}$.

Because of the missing atoms, the (linear) scaling symmetry by a factor τ is only locally verified. Nevertheless, there is a large number of Fibonacci lines within the decagonal plane that have such linear, but slightly broken, scaling symmetry (see Fig. 8). This is a likely explanation for the scale invariance by a factor τ of the positions of the Bragg peaks mentioned above.

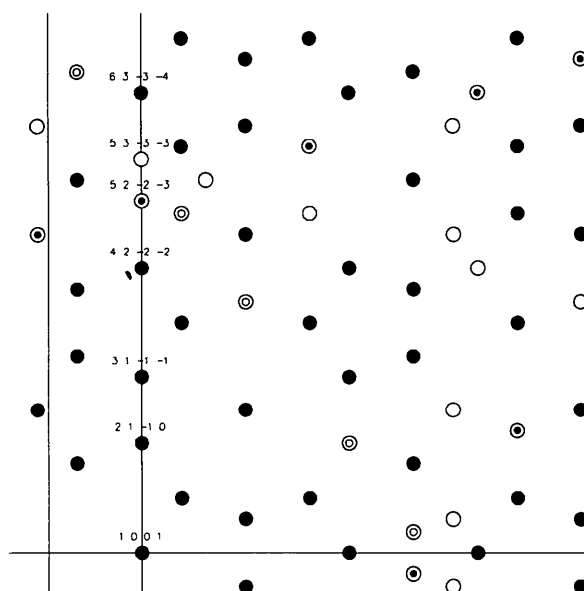
This insight gives the idea of investigating the transformations of the type $1_2 \oplus N_1^k \oplus 1$ that have integral entries when expressed with respect to the d basis, since they leave the p positions invariant and induce in space a linear scaling by a factor τ^k . One finds that the lowest value for which these requirements are satisfied is $k=3$. One has accordingly

$$\begin{aligned} T_2(d) &= \begin{pmatrix} 2 & 1 & -1 & -1 & 0 \\ 1 & 1 & 0 & -1 & 0 \\ -1 & 0 & 1 & 1 & 0 \\ -1 & -1 & 1 & 2 & 0 \\ 0 & 0 & 0 & 0 & 1 \end{pmatrix} \\ &= T_2 \sim 1_2 \oplus N_1^3 \oplus 1, \end{aligned} \quad (28)$$

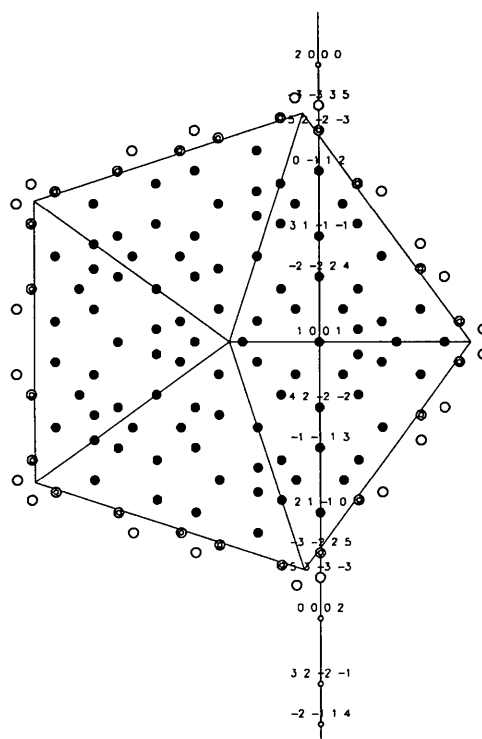
which yields a new symmetry generator of the $Al_{78}Mn_{22}$ quasicrystal phase,

$$g_6 = \{T_2 | 0, 0, 0, 0, 0\}. \quad (29)$$

Note that this point-group element leaves the decagonal plane invariant. In such a plane it represents a τ^3 dilatation along a Fibonacci line parallel to the (vertical) y axis, with origin on the (horizontal) x axis. In particular, the position (1001) is left invariant by $g_6 = \{T_2 | 0, 0, 0, 0, 0\}$, whereas the position (21 $\bar{1}$ 0) is transformed to (63 $\bar{3}\bar{4}$), which has ordinate τ^3 times the ordinate of (21 $\bar{1}$ 0). If applied to (2100) one then gets (53 $\bar{2}\bar{3}$), as expected [see Figs. 1(b) and 7(a)].



(a)



(b)

Fig. 7. A Fibonacci chain through the position (1001). (a) Not all the points of the Fibonacci chain indicated in Fig. 5 are occupied here. [For comparison take into account that in Fig. 5 the origin is at (0000).] This is an effect of the boundaries of the crystal form $CF_1^{(1)}$, as shown in (b). (b) The positions belonging to the Fibonacci chain that are indicated in Fig. 5 but missing in (a) are external to the crystal form, as expected.

In an analogous way, one finds that

$$T_{10}(d) = \begin{pmatrix} 0 & -1 & -1 & -1 & 0 \\ 1 & 3 & 2 & 1 & 0 \\ 1 & 2 & 3 & 1 & 0 \\ -1 & -1 & -1 & 0 & 0 \\ 0 & 0 & 0 & 0 & 1 \end{pmatrix}$$

$$= T_{10} \sim N_1^3 \oplus 1_2 \oplus 1 \quad (30)$$

leaves the Σ lattice invariant and interchanges the p positions according to the permutation (1243), which is the inverse of that produced by S_{10} . Thus the p positions are left invariant by the product $T_{10}S_{10} = T_0$ and we have found a new symmetry element

$$g_7 = \{T_0 | 0, 0, 0, 0, 0\} \quad (31)$$

with

$$T_0(d) = \begin{pmatrix} 0 & -1 & -2 & -1 & 0 \\ 2 & 4 & 4 & 1 & 0 \\ 1 & 4 & 4 & 2 & 0 \\ -1 & -2 & -1 & 0 & 0 \\ 0 & 0 & 0 & 0 & 1 \end{pmatrix}$$

$$= T_0 \sim N_1^4 \oplus N_1 \oplus 1. \quad (32)$$

Furthermore, $T_{10}^2 = T$ permutes the p positions in the same way as R and S and it also yields a symmetry element

$$g_8 = \{T | 0, 0, 0, 0, \frac{1}{2}\} = T_{1/2}. \quad (33)$$

In contrast to S , the transformation T is a linear scaling operation in the decagonal plane and not a two-dimensional one. Combining T with the total inversion I_1 in the subspace (D_1, D_2) , which can be expressed as

$$\{I_1 | 0, 0, 0, 0, \frac{1}{2}\} = \{m_1 R^5 | 0, 0, 0, 0, \frac{1}{2}\} \sim g_2 g_5^5, \quad (34)$$

one obtains a new symmetry T_1 of the quasicrystal,

$$g_9 = \{I_1 T | 0, 0, 0, 0, 0\} = T_1. \quad (35)$$

In the decagonal plane, T_1 corresponds to a mirror transformation combined with a linear scaling transformation, in a direction perpendicular to that expanded by T_2 . Indeed, the positions (2100) , $(32\bar{1}\bar{1})$, $(53\bar{2}\bar{3})$ are mapped by T_1 into $(065\bar{2})$, $(174\bar{3})$ and $(383\bar{5})$, respectively. The scaling factor is $-\tau^6$ with respect to the distance from the vertical line through the origin (the y axis), which is the invariant line. In particular, the position $(220\bar{1})$ is transformed into $(30\bar{2}0)$, as expected. (See, for example, Figs. 3 and 11.)

4.3. Local tenfold axes

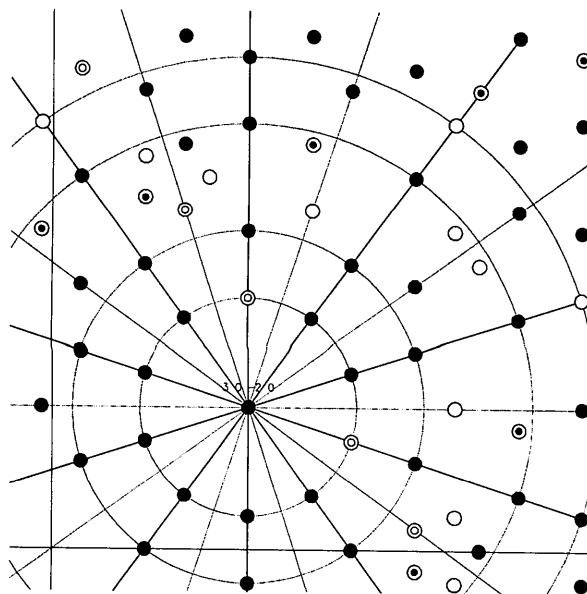
The analysis given in the previous subsection allows one to understand the origin of an impressive structural features of the decagonal phase: a circular

arrangement of ten atoms around a central one, situated at a tenfold axis of local point symmetry. More will be said later on about the distribution of these local tenfold axes. Here an explanation will be given of how such local symmetry is possible, despite the fact that the decagonal plane has only fivefold symmetry.

In a way analogous to the scaling symmetry by τ considered above, the 36° rotation R given in (9) interchanges the p positions, according to the permutation (14)(23) and leaves the five-dimensional lattice Σ invariant. In contrast, the p -independent sublattice Λ_2 generated by D_3, D_4 is not left invariant. Its projection in the physical space is a one-dimensional rank-two \mathbb{Z} -module F_2 along a Fibonacci line, which is p independent, as already explained. Therefore, a Fibonacci line is transformed by R into a rotated one, arising from $\pi R \Lambda_2$.

The crystal form CF_I , however, is not R invariant, so the occupied Fibonacci positions along those lines do not always show such a point symmetry. Nevertheless, around points sufficiently inside the form CF_I , a local tenfold symmetry arises. One could equally well describe the situation in terms of a fivefold point symmetry around a local center of inversion of the Fibonacci chains involved.

A typical example is shown in Fig. 8, where one sees that, despite the local character, the rotational symmetry goes well beyond the nearest neighbors. For peripheral atomic positions, the situation is in principle analogous, but is structurally unphysical due to too many missing atoms.



4.4. Involutions

The sublattice A_1 , generated by D_1 and D_2 , is left invariant by the reflection $m_0: D_1 \leftrightarrow D_2$ and by the hyperbolic rotation N_1^2 , as we have seen. Accordingly, one obtains two infinite families of two-dimensional hyperbolic mirrors, as already discussed by Janner & Ascher (1969),

$$m_k = N_1^{2k} m_0 \quad \text{and} \quad r_k = -N_1^{2k} m_0, \quad k \in \mathbb{Z}. \quad (36)$$

Expressed in the D basis, one typically has

$$m_k(D) = \begin{pmatrix} -f_{2k} & -f_{2k-2} \\ f_{2k+2} & f_{2k} \end{pmatrix}, \quad (37)$$

where f_k is the k th Fibonacci number, which is also defined, by recursion, for negative k values, $f_{|k|} = (-1)^{|k|+1} f_{|k|}$.

A set of hyperbolic mirrors m_k and r_k together with their action on some of the positions with $p=2, 3$ are indicated in Fig. 9. We recall that a hyperbolic mirror reflects a point on the invariant line along a direction that is symmetric with respect to the 45° asymptote. (The asymptote is thus the bisecting line of the previous two directions.) The product of two successive reflections generates the hyperbolic rotation N_1^2 ,

$$m_{k+1} m_k = r_{k+1} r_k = N_1^2, \quad \text{for any } k \in \mathbb{Z}. \quad (38)$$

Analogous considerations can be made for the sublattice A_2 , generated by D_3 and D_4 , which is equivalent to A_1 since it arises from the latter by a

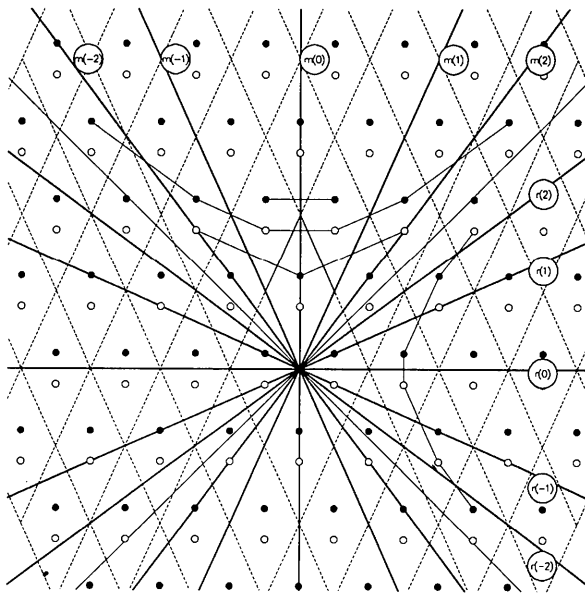


Fig. 9. A set of the infinite family of hyperbolic mirrors leaving invariant the sublattice A_1 and their action on the atomic positions at $p=2$ and $p=3$ as in Fig. 4(b). The product of two mirrors generates a hyperbolic rotation (or rotation-inversion) producing a transformation in space with a positive (or negative) scaling factor.

hyperbolic rotation, which is the Euclidization considered in Fig. 6. With respect to the basis D_3, D_4 one then has, starting from the reflection $m'_0: D_3 \rightarrow D_3 - D_4$ and $D_4 \rightarrow -D_4$:

$$m'_k(D) = (N'_1)^{2k} m'_0 = \begin{pmatrix} f_{2k-1} & -f_{2k} \\ f_{2k-2} & -f_{2k-1} \end{pmatrix}$$

and

$$r'_k = -m'_k. \quad (39)$$

A set of these hyperbolic mirrors is shown in Fig. 10. One can now combine a mirror in the (D_1, D_2) plane with another one in the (D_3, D_4) plane, obtaining in this way a five-dimensional involution. (An involution is a symmetry transformation having eigenvalues ± 1 .) Not all combinations are allowed, as the lattice Σ is centered with respect to the lattice generated by the D basis. Examples of allowed combinations, giving involutions that leave the decagonal lattice Σ invariant are:

$$\begin{aligned} m_k \oplus m'_{k-1} \oplus 1, \quad m_k \oplus m'_{k+2} \oplus 1, \quad m_k \oplus r'_{k+2} \oplus 1, \\ r_k \oplus r'_{k-1} \oplus 1, \quad r_k \oplus r'_{k+2} \oplus 1, \quad r_k \oplus m'_{k+2} \oplus 1, \dots \end{aligned} \quad (40)$$

To simplify the notation, let

$$\hat{m}_k = m_k \oplus m'_{k-1} \oplus 1 \quad \text{and} \quad \hat{r}_k = r_k \oplus r'_{k-1} \oplus 1, \quad (41)$$

which have the properties

$$S \hat{m}_k = \hat{m}_{k+1}, \quad S \hat{r}_k = \hat{r}_{k+1} \quad \hat{m}_{k+1} \hat{m}_k = \hat{r}_{k+1} \hat{r}_k = S. \quad (42)$$

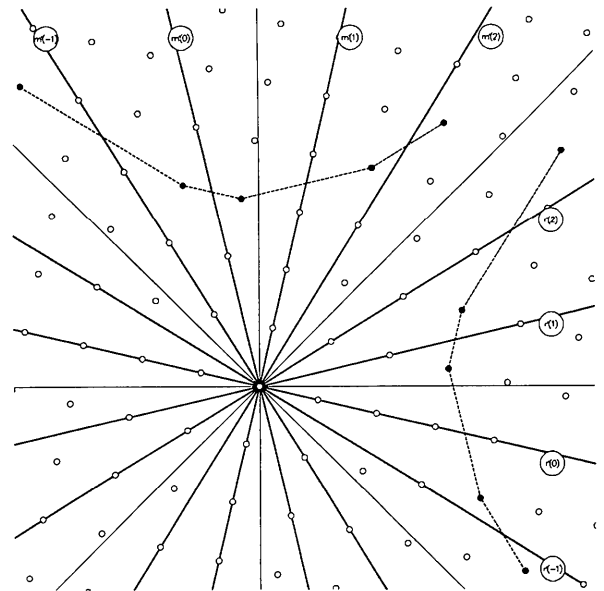


Fig. 10. As in Fig. 9, for the sublattice A_2 . The corresponding mirrors are the same but they appear in a different orientation because they are transformed by the hyperbolic rotation with angle $\beta = -\tanh^{-1}(5^{1/2} - 2)$ as indicated in Fig. 6.

As an illustration consider

$$\hat{m}_4(D) = \begin{pmatrix} \bar{2}\bar{1} & \bar{8} & 0 & 0 & 0 \\ 55 & 21 & 0 & 0 & 0 \\ 0 & 0 & 5 & \bar{8} & 0 \\ 0 & 0 & 3 & \bar{5} & 0 \\ 0 & 0 & 0 & 0 & 1 \end{pmatrix}, \quad (43)$$

$$\hat{m}_3(D) = \begin{pmatrix} \bar{8} & \bar{3} & 0 & 0 & 0 \\ 21 & 8 & 0 & 0 & 0 \\ 0 & 0 & 2 & \bar{3} & 0 \\ 0 & 0 & 1 & \bar{2} & 0 \\ 0 & 0 & 0 & 0 & 1 \end{pmatrix},$$

so the relations

$$\hat{m}_4\hat{m}_3 = S \quad \text{and} \quad \hat{m}_4^2 = \hat{m}_3^2 = 1 \quad (44)$$

can be checked.

In fact, from results found so far, it seems that all the allowed involutions are generated by \hat{m}_k , by the two two-dimensional inversions I_1 and I_2 of the lattices A_1 and A_2 , respectively, combined with the linear scalings T_0 , T_1 and T_2 considered above. Note that the two inversions may be expressed by point-group elements indicated earlier: I_2 is the Euclidean mirror m_1 given in (10) and I_1 corresponds to $-m_1 = R^5 m_1$ with R as in (9). In summary, we have the relations

$$\{I_1|0, 0, 0, 0, \frac{1}{2}\} \sim g_2 g_1^5, \quad \{I_2|0, 0, 0, 0, 0\} = g_2, \quad (45)$$

$$\{I|0, 0, 0, 0, \frac{1}{2}\} \sim g_1^5.$$

If one now considers the action of all these involutions on the atomic positions one sees that the p values are left invariant by \hat{m}_k for k even and permuted according to (14)(23) for k odd (see Fig. 9). In the first case the nonprimitive translation required to leave the decagonal structure invariant is equivalent to zero and in the second case it is $c/2$. Thus, we get the additional symmetry generators

$$g_{10} = \{\hat{m}_0|0, 0, 0, 0, 0\} = \hat{m}_0, \quad (46)$$

$$g_{11} = \{\hat{m}_1|0, 0, 0, 0, \frac{1}{2}\} = \hat{c}_1. \quad (47)$$

For the involutions \hat{r}_k it is just the other way around, as one can also see from Fig. 9. In this case, we have

$$\{\hat{r}_0|0, 0, 0, 0, \frac{1}{2}\} \sim g_1^5 g_{10} \quad (48)$$

and

$$\{\hat{r}_1|0, 0, 0, 0, 0\} \sim g_1^5 g_{11}.$$

Examples of structural relations that are consequences of these non-Euclidean symmetry transformations are given later (see Tables 2 and 3).

4.5. Invariant Minkowskian metric

The transformations S , T , \hat{m}_0 , \hat{m}_1 , I_1 , $I_2 = m_1$ and m_2 generate a point group K_m that leaves invariant an

Table 2. Images of the five atomic positions closest to the origin in the decagonal plane of atom 1, under some elements of the Minkowskian point group K_{0m}

| 1 | m_1 | S^2 | \hat{m}_4 | $T_2^2 \hat{m}_2$ | T_1 | TS^{-1} |
|------------|------------|------------------------------|------------------------------|------------------------------|---------------------------------|------------------------------|
| 2, 1, 0, 0 | 0, 0, 1, 2 | 8, 3, 5, $\bar{5}$ | 0, 6, 5, $\bar{2}$ | 3, 3, 0, $\bar{2}$ | 0, 6, 5, $\bar{2}$ | 2, $\bar{1}$, $\bar{1}$, 2 |
| 1, 2, 1, 0 | 0, 1, 2, 1 | 3, 8, 3, $\bar{5}$ | 0, $\bar{2}$, 0, 3 | $\bar{3}$, $\bar{2}$, 3, 5 | 6, $\bar{1}$, $\bar{1}$, 2, 5 | $\bar{1}$, 6, 5, $\bar{1}$ |
| 0, 1, 2, 1 | 1, 2, 1, 0 | $\bar{5}$, 3, 8, 3 | 3, 0, $\bar{2}$, 0 | 5, 3, $\bar{2}$, $\bar{3}$ | 5, $\bar{1}$, $\bar{1}$, 6 | $\bar{1}$, 5, 6, $\bar{1}$ |
| 0, 0, 1, 2 | 2, 1, 0, 0 | 5, $\bar{5}$, 3, 8 | $\bar{2}$, 5, 6, 0 | $\bar{2}$, 0, 3, 3 | $\bar{2}$, 5, 6, 0 | 1, $\bar{1}$, $\bar{1}$, 2 |
| 1, 0, 0, 1 | 1, 0, 0, 1 | 3, $\bar{5}$, $\bar{5}$, 3 | 3, $\bar{5}$, $\bar{5}$, 3 | 1, 0, 0, 1 | 5, 16, 16, $\bar{5}$ | 3, $\bar{5}$, $\bar{5}$, 3 |

Table 3. Image of the atom 1 position $P = (2100)$ in the decagonal plane, under some elements of the multimetric point group K_0

| $m_1 \hat{m}_4$ | $\hat{m}_3 m_2$ | $m_2 \hat{m}_3$ | SR^{-1} | SR | $\hat{m}_3 R^{-1}$ | $\hat{m}_2 R$ |
|---------------------|-----------------------------|---------------------|---------------------|--------------------|---------------------|------------------------------|
| $\bar{2}$, 5, 6, 0 | 1, 2, 1, 0 | $\bar{1}$, 1, 3, 2 | 3, 0, $\bar{2}$, 0 | 3, 3, 0, $\bar{2}$ | 0, 1, 2, 1 | 2, $\bar{1}$, $\bar{1}$, 1 |
| $m_2 S$ | T_2 | $T_2 \hat{m}_2$ | T_0 | $T_1 T_2$ | $T_1^{-1} T_0$ | $T_1^{-1} T_2$ |
| 0, $\bar{2}$, 0, 3 | 5, 3, $\bar{2}$, $\bar{3}$ | 1, 2, 1, 0 | 3, 0, $\bar{2}$, 0 | 3, 8, 3, $\bar{5}$ | 2, 0, $\bar{2}$, 0 | 3, 4, $\bar{1}$, $\bar{5}$ |

indefinite metric tensor suitably defined in the five-dimensional superspace. One can verify this by considering in the superspace instead of the orthonormal basis e_1, \dots, e_5 the indefinite basis $\varepsilon_1, \dots, \varepsilon_5$ with $\varepsilon_1^2 = \varepsilon_2^2 = \varepsilon_5^2 = 1$, $\varepsilon_3^2 = \varepsilon_4^2 = -1$ and $\varepsilon_i \varepsilon_k = 0$ for $i \neq k$. According to Klein (1892), K_m is a group of pseudo-Euclidean transformations. However, it can also be described as a Minkowskian group. The transformations T_0 and T_2 have been omitted from the generators; they are neither hyperbolic rotations nor involutions. In the subspace (D_3, D_4) they correspond to the negautomorphs N_1 and N_1^3 , respectively, giving rise in the five-dimensional space to a situation requiring the concept of a multimetric space group (Janner, 1991b, c). The application of these ideas to the $\text{Al}_{78}\text{Mn}_{22}$ quasicrystal structure will be discussed in the next section. Furthermore, from the generators indicated, one sees that there are symmetries leaving both the Euclidean and the Minkowskian metric tensors invariant.

The lattice Σ of symmetry translations remains the same. This fixes the relative orientation of the two bases, which is not free. For the validity of the superspace approach it is essential to require that, by the embedding of the quasicrystal structure, rotations remain rotations, whereas hyperbolic rotations yield scaling transformations. For the decagonal phase $\text{Al}_{78}\text{Mn}_{22}$, this is indeed the case and the d basis can be expressed with respect to both the positive definite and the indefinite orthonormal bases:

$$d_k = \frac{2}{5} a [(c_k - 1) e_1 + s_k e_2 + (c_{2k} - 1) e_3 + s_{2k} e_4] \quad (49)$$

$$= \frac{2}{5} a [(c_k - c_{2k}) \varepsilon_1 + (s_k - s_{2k}) \varepsilon_2 + (c_k + c_{2k} - 2) \varepsilon_3 + (s_k + s_{2k}) \varepsilon_4], \quad k = 1, \dots, 4$$

and

$$d_5 = c\varepsilon_5 = c\varepsilon_5,$$

where $c_k = \cos(2\pi k/5)$ and $s_k = \sin(2\pi k/5)$.

The elements $g_2, g_4, g_5, g_8, g_9, g_{10}$ and g_{11} together with the lattice translations generate the five-dimensional Minkowskian space group

$$G_m = PS_3 T_1 T_1 / m_z m_1 \hat{m}_0 \hat{c}_1. \quad (50)$$

As in the case of the Euclidean symmetry elements, to verify the structural relevance of these pseudo-Euclidean symmetries we consider the point group K_{0m} of the symmetry transformations that leave a decagonal plane invariant, in particular that of atom 1, omitting as usual the fifth coordinate and taking into account the shift of the origin by $f = (\frac{4}{5}, \frac{4}{5}, \frac{4}{5}, \frac{4}{5})$ and the symmetry-breaking effects of the crystal form $CF_S^{(1)}$ for this set of positions. The point group K_{0m} is generated by $\hat{m}_0, m_1, T_1, T_2^2, TS$ and S^2 . As starting points, we take the five atomic positions closest to the origin and apply to them elements of K_{0m} . The results are given in Table 2.

The nature of the transformation S^2 in space is an inflation by $\tau^4 \approx 6.854$, that of T_2 is a linear scaling by τ^3 along the y axis with the x axis as an invariant line, thus the transformation T_1 scales along the x direction, by a factor $-\tau^6$ the distance from the y axis, whereas the effect of \hat{m}_0 in the physical space is less evident, even if expressible in terms of scaling and rotation.

5. Multimetric symmetry

Both the Euclidean space group G_e and the pseudo-Euclidean (or Minkowskian) group G_m are symmetry groups of the embedded quasicrystal. They share the lattice of symmetry translations, for which a positive definite and an indefinite invariant metric have been defined for the lattice basis d_1, \dots, d_5 given in (49). In addition, we have symmetry elements g_6 and g_7 , defined in (29) and (31), respectively, which are neither Euclidean nor pseudo-Euclidean but satisfy the multimetric requirement as given in equation (8) of Janner (1991c). Thus a multimetric formulation for the symmetry of $Al_{78}Mn_{22}$ is justified.

One starts with a set of diagonal metric tensors involving ± 1 only, attached to the five-dimensional superspace that is considered, at first, as an affine space. There are therefore in total 2^5 different metric tensors. In the present case, however, in addition to the Euclidean metric tensor $g_0^0 = (1, 1, 1, 1, 1)$ we can restrict consideration to the eight tensors

$$\begin{aligned} g_1^0 &= (1, 1, \bar{1}, \bar{1}, 1), & g_2^0 &= (\bar{1}, \bar{1}, 1, 1, 1), \\ g_3^0 &= (1, \bar{1}, \bar{1}, 1, 1), & g_4^0 &= (\bar{1}, 1, 1, \bar{1}, 1), \\ g_5^0 &= (\bar{1}, 1, 1, 1, 1), & g_6^0 &= (1, \bar{1}, \bar{1}, 1, 1), \\ g_7^0 &= (1, 1, \bar{1}, 1, 1), & g_8^0 &= (1, 1, 1, \bar{1}, 1), \end{aligned} \quad (51)$$

where the corresponding diagonal elements are indicated. As an affine basis for the lattice Σ the one expressed in terms of the orthonormal ε_i basis may

be chosen. The matrix α fixing the relation to the lattice basis d_1, \dots, d_5 is defined by

$$d_i = \sum_{j=1}^5 \varepsilon_j \alpha_{ji}, \quad (52)$$

and takes the form

$$\alpha = \frac{2a}{5} \begin{pmatrix} \tau-1/2 & -\tau+1/2 & -\tau+1/2 & \tau-1/2 & 0 \\ \frac{(7-4\tau)^{1/2}}{2} & \frac{(3+4\tau)^{1/2}}{2} & \frac{-(3+4\tau)^{1/2}}{2} & \frac{-(7-4\tau)^{1/2}}{2} & 0 \\ -5/2 & -5/2 & -5/2 & -5/2 & 0 \\ \frac{(3+4\tau)^{1/2}}{2} & \frac{-(7-4\tau)^{1/2}}{2} & \frac{-(7-4\tau)^{1/2}}{2} & \frac{-(3+4\tau)^{1/2}}{2} & 0 \\ 0 & 0 & 0 & 0 & 5c/2a \end{pmatrix} \quad (53)$$

Corresponding to the metric g_ν^0 , there is now a whole set $g(\Sigma)$ of so-called compatible metric tensors g_ν^d defining different scalar products for the basis vectors d_i and satisfying

$$g_\nu^d = \tilde{\alpha} g_\nu^0 \alpha, \quad \nu = 1, \dots, 8, \quad (54)$$

where the tilde denotes the transposed matrix. In particular, one obtains the well known form for the Euclidean metric tensor of the d basis

$$g_e = g_0^d = \frac{4a^2}{5} \begin{pmatrix} 2 & 1 & 1 & 1 & 0 \\ 1 & 2 & 1 & 1 & 0 \\ 1 & 1 & 2 & 1 & 0 \\ 1 & 1 & 1 & 2 & 0 \\ 0 & 0 & 0 & 0 & 5c^2/4a^2 \end{pmatrix} \quad (55)$$

and the metric tensor corresponding to the Minkowskian case $(1, 1, \bar{1}, \bar{1}, 1)$

$$g_m = g_1^d = \frac{4a^2}{25} \begin{pmatrix} -2\tau-3 & \tau-8 & -\tau-7 & 2\tau-6 & 0 \\ \tau-8 & 2\tau-6 & -2\tau-3 & -\tau-7 & 0 \\ -\tau-7 & -2\tau-3 & 2\tau-6 & \tau-8 & 0 \\ 2\tau-6 & -\tau-7 & \tau-8 & -2\tau-3 & 0 \\ 0 & 0 & 0 & 0 & 25c^2/4a^2 \end{pmatrix}. \quad (56)$$

Analogous expressions can be derived for the other metric tensors. The Euclidean point-group elements E and the Minkowskian elements M satisfy the usual metrical invariance property

$$\tilde{E} g_e E = g_e, \quad \tilde{M} g_m M = g_m, \quad (57)$$

whereas for the transformations T_0 and T_2 , given in (32) and (28), respectively, pairs of different metric tensors are involved:

$$\tilde{T}_0 g_1^d T_0 = g_3^d \quad \text{and} \quad \tilde{T}_0 g_3^d T_0 = g_1^d; \quad (58)$$

$$\tilde{T}_2 g_6^d T_2 = g_8^d \quad \text{and} \quad \tilde{T}_2 g_8^d T_2 = g_6^d. \quad (59)$$

Other pairs of metric tensors are involved when

considering transformations like S_{10} and T_{10} . In this way one verifies that the point group K generated by

$$K = \{m_1, m_2, m_z, T, T_2, \hat{m}_0, \hat{m}_1\} \quad (60)$$

is indeed a multimetrical point group with respect to $g(\Sigma)$. It follows that the group- G subgroup of the affine group $A(5)$,

$$G = \{\Sigma, g_1, \dots, g_{11}\}, \quad (61)$$

is also a multimetrical space group with $\Sigma, g_1, \dots, g_{11}$ given in previous equations.

Since the product of two symmetry transformations is also a symmetry transformation, one expects that the product of a Euclidean and a non-Euclidean symmetry transformation also leaves the structure invariant. This is indeed the case and is a nontrivial observation since such elements are structurally relevant for the occupied positions in space and not only for the ideal ones of the infinite supercrystal. For a practical verification, we consider the subgroup G_0 of G that leaves a decagonal plane invariant. This group is symmorphic and its point group K_0 is of infinite order. A full analysis of the properties of G and of G_0 is beyond the aim of the present paper. Here the analysis is limited to an indication that indeed the atom 1 positions within a decagonal plane are left invariant by a number of the generators given above (taking possible symmetry-breaking effects of the crystal form $\text{CF}_S^{(1)}$ into account). The Euclidean symmetries have already been considered in Table 1.

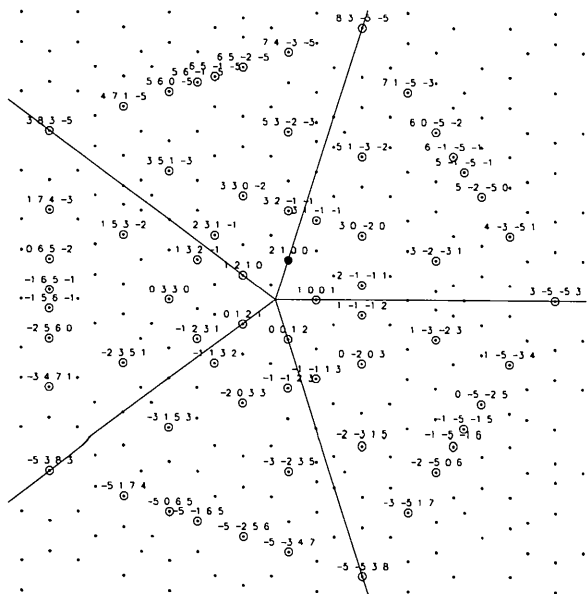


Fig. 11. The atomic positions occupied by atom 1 are as in Figs. 3 and 2(b). Those encircled can be obtained by applying to the position (2100) elements of the point-symmetry group of the decagonal plane. Only a subset of these point-group-equivalent positions is marked here. (Some more points can be seen in Fig. 15).

Some of the Minkowskian ones are given in Table 2, whereas additional typical multimetrical point-group transformations appearing in K_0 can be found in Table 3.

In Fig. 11 the occupied atomic positions that one obtains by applying elements of the point group K_0 to the atomic position $P = (2100)$ are circled. The general behavior clearly reveals pentagrammatic symmetry, even if not all K_0 -equivalent atomic positions are shown. We recall that all the positions appearing in Fig. 11 are translationally equivalent.

6. Pentagrammatic symmetry

The aim of this section is to discuss in what sense the point group K_0 , i.e. the symmetry of the atom 1 positions belonging to a decagonal plane, is an invariance group of self-similar pentagrams. Before doing that, let us consider the \mathbb{Z} -module $M_0 = \{a_1, \dots, a_4\}$ obtained from M by omitting the basis element a_5 , which is not relevant in the present context. Furthermore, the action of K_0 is also restricted to the constant- z plane.

The point group K_0 leaving the set of translationally equivalent positions invariant also leaves M_0 invariant. The particular multimetrical character of K_0 in the superspace implies that in the decagonal plane its elements are expressible as products of (two-dimensional) rotations, proper and improper, and scaling transformations with positive as well as negative scaling factors. Accordingly, the name 'scale-rotational point group' is justified.

In previous publications (Janner, 1990; Janner & Janssen, 1990), a scale-rotational point group was defined as a subgroup of the group $H(m)$ of homotheties of a Euclidean m -dimensional space V . We recall that $H(m)$ consists of elements of the type

$$\alpha = (\lambda, R) \in H(m), \quad \lambda \in \mathbb{R}, R \in O(m) \quad (62)$$

acting on the vectors r of V according to

$$\alpha r = \lambda Rr, \quad (\lambda, R) \in H(m). \quad (63)$$

In the present case, however, K_0 is not a subgroup of $H(2)$ since it contains, together with planar scalings (with respect to an invariant point), linear scalings (having an invariant line).

We define, therefore, as an m -dimensional full group of homotheties $H_F(m)$ the group generated by the subgroups $H(m), H(m-1), \dots, H(1)$,

$$H_F(m) = \{H(m), H(m-1), \dots, H(1)\}, \quad (64)$$

where $H(k)$ acts on a k -dimensional subspace leaving the orthocomplementary subspace pointwise invariant. The group H_F is independent of the particular choice made for these subspaces. For the present case we have

$$K_0 \subset H_F(2) \quad \text{and} \quad K_0 M_0 = M_0. \quad (65)$$

This is a property of the symmetries considered here for the decagonal phase and is not true in general, as multimetric symmetries are also structurally possible in the physical space (Janner, 1991a).

Consider now a self-similar pentagram, obtained by extending the classical construction by repeated inflations and deflations. Starting from a regular pentagon with edge l and vertices $1, \dots, 5$ joining alternative vertices (say 1-3, 2-4, 3-5, 4-1), one obtains a smaller regular pentagon having an edge l/τ turned by 36° with respect to the previous one (deflation). Conversely, a larger one (with edge $l\tau$) is obtained through lengthening the edges of the original pentagon, by joining successive intersections (inflation).

Looking at such self-similar pentagrams, one immediately recognizes among the elements of K_0 those that are symmetries of the set of vertices of all inflated/deflated pentagrams (Fig. 12), such as the rotation R^2 , the mirror $m_1 = m_y$, the τ^4 scaling S^2 , the rotation-scale $RS = SR$, the scale-inversion $\bar{I}S$ and the mirror-scale $m_2S = Sm_2$. It is, therefore, not surprising that the point-group equivalent positions indicated in Fig. 11 show pentagrammatic symmetry.

Less evident symmetries are also present, such as the linear τ^6 scaling T_1 , which is a reflection in the y axis combined with a dilation along the x axis by a factor τ^6 or the other linear scaling T_2 (Fig. 13). These transformations introduce additional points. Such additional points are also present in the Fourier map as positions of the atoms in a decagonal plane, once the various pentagrams have been drawn (Fig. 14). In any case, the full set of (occupied) positions that are K_0 equivalent to a given one, say $P = (2100)$,

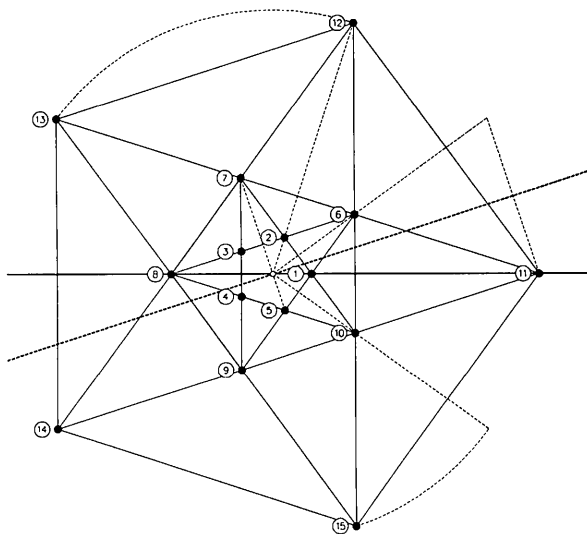


Fig. 12. Typical multimetric superspace-symmetry transformations that induce, in the two-dimensional plane, scaling-rotation transformations that leave a self-similar pentagram invariant. Illustrated are: R^2 : 12 \rightarrow 13; S^2 : 2 \rightarrow 12; m_1 : 13 \rightarrow 14; m_2S : 6 \rightarrow 11; $\bar{I}S$: 5 \rightarrow 7; RS^{-1} : 15 \rightarrow 10.

lie along straight lines through the edges of the entire set of self-similar pentagrams. Furthermore, the local tenfold axes are located at the vertices of the pentagrams, whereas it is along the edges that one finds the corresponding sets of intersecting Fibonacci lines (Fig. 15).

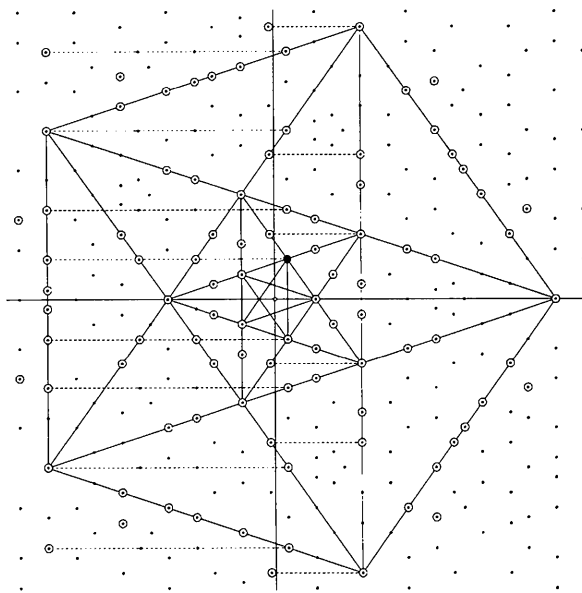


Fig. 13. A set of point-group-equivalent positions occupied by atom 1 showing pentagrammatic symmetry (compare with Fig. 11). In particular, the effect of the linear scaling transformation T_1 on positions along Fibonacci lines (parallel to the invariant one) is shown. Connected by dashed lines are pairs of equivalent positions that one obtains by combining a reflection in the y axis with a τ^6 dilation along the x axis.

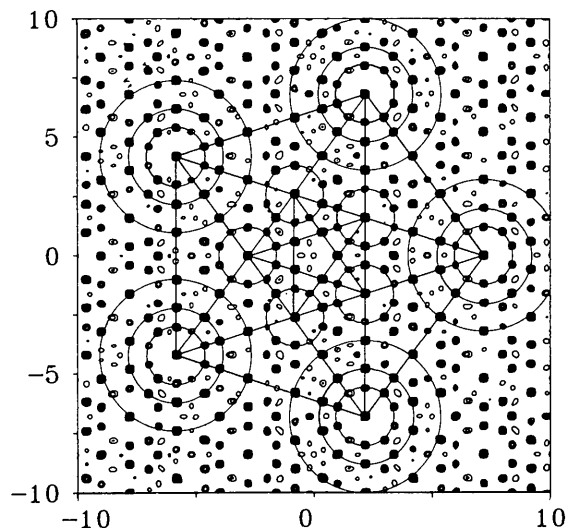


Fig. 14. The structural relevance of the pentagrammatic symmetry is demonstrated on the basis of the Fourier map of a decagonal plane of $Al_{78}Mn_{22}$ obtained by W. Steurer, who provided this figure. Compare with Figs. 13 and 15.

7. Decagrammatic point group

The point group K of the nonsymmorphic multi-metrical space group G was given in (60). Its planar subgroup K_0 is of index four in K and the coset decomposition is

$$K = K_0 + m_z K_0 + m_2 K_0 + m_z m_2 K_0, \quad (66)$$

with m_2 and m_z given as in (11) and (12), respectively.

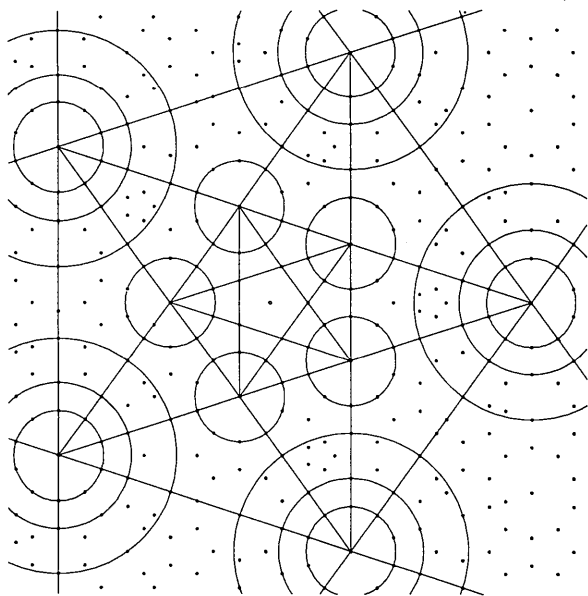


Fig. 15. The local tenfold axes are primarily situated at the vertices of a self-similar pentagram, whereas the corresponding Fibonacci lines appear along the edges. Compare with Fig. 14 for the experimental atomic positions.

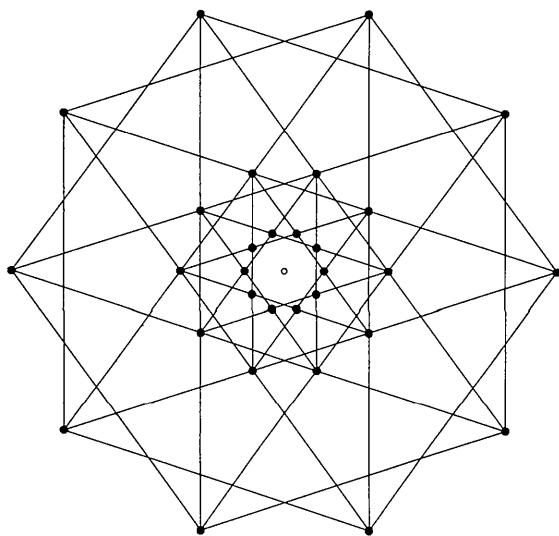


Fig. 16. The point-group symmetry of a self-similar decagram is obtained by adding the total inversion to the point-group symmetry of a self-similar pentagram.

Indeed, one finds in K_0 the elements m_1 , RS , \hat{m}_0 and T_2 . One obtains R from $m_2 m_1 = R$ and thus also S ; together with $S \hat{m}_0 = \hat{m}_1$ one obtains a set of generators for K .

Applying the transformation R to a self-similar pentagram, one generates a self-similar decagram (Fig. 16). Therefore, the point group K is the invariance group of a self-similar decagram, supplemented by the five-dimensional total inversion (or by the mirror plane m_z). This concludes the present analysis, which is not necessarily exhaustive.

While trying to present in a clear way the relations between symmetries and structural features, new symmetry elements have been identified repeatedly. Thus the true point group may be larger than the one indicated here. Nevertheless, it is likely that the most relevant crystallographic symmetries of the $\text{Al}_{78}\text{Mn}_{22}$ decagonal quasicrystal phase have been given here. These symmetries were not apparent despite the fact that the structural characterization given by Steurer (1991), Ishihara & Yamamoto (1988) and Yamamoto & Ishihara (1988) of that compound in terms of a Penrose-like pattern is in principle complete.

The partial support of the Stichting FOM of the Dutch National Science Foundation NWO is gratefully acknowledged. I should like to thank especially Dr W. Steurer for having put at my disposal the drawings of the five-dimensional Fourier synthesis. Thanks are also expressed to the two referees for their help in improving the original manuscript.

References

- BAK, P. (1985). *Phys. Rev. B*, **32**, 5764–5772.
- ISHIHARA, K. N. & YAMAMOTO, A. (1988). *Acta Cryst.* **A44**, 508–516.
- JANNER, A. (1990). In *Geometry and Thermodynamics. Common Problems of Quasi-Crystals, Liquid Crystals and Incommensurate Systems*, edited by J.-C. TOLÉDANO, pp. 49–65. New York, London: Plenum Press.
- JANNER, A. (1991a). *Phys. Rev. Lett.* **67**, 2159–2162.
- JANNER, A. (1991b). *Acta Cryst.* **A47**, 577–590.
- JANNER, A. (1991c). *Phys. Rev. B*, **43**, 13206–13214.
- JANNER, A. (1992). *Phase Transit.* In the press.
- JANNER, A. & ASCHER, E. (1969). *Z. Kristallogr.* **130**, 277–303.
- JANNER, A. & JANSSEN, T. (1990). In *Quasicrystals and Incommensurate Structures in Condensed Matter*, edited by J. M. YACAMÁN, D. ROMEU, V. CASTAÑO & A. GÓMEZ, pp. 96–108. Singapore: World Scientific.
- JANSSEN, T. (1986). *Acta Cryst.* **A42**, 261–271.
- JANSSEN, T. (1988). *Phys. Rep.* **168**, 57–113.
- KATZ, A. & DUNEAU, M. (1986a). *J. Phys. (Paris) Colloq.* **47**, C3, 103–113.
- KATZ, A. & DUNEAU, M. (1986b). *J. Phys. (Paris)*, **47**, 181–196.
- KLEIN, F. (1892). *Vorlesungen über nicht Euklidische Geometrien*. Berlin: Springer (1928). Reprint, New York: Chelsea (1959).
- KURIYAMA, M. & LONG, G. G. (1986). *Acta Cryst.* **A42**, 164–172.
- LONG, G. G. & KURIYAMA, M. (1986). *Acta Cryst.* **A42**, 156–164.
- OSTLUND, S. & WRIGHT, D. C. (1986). *Phys. Rev. Lett.* **56**, 2068–2071.
- STEINHARDT, P. J. & OSTLUND, S. (1987). *The Physics of Quasicrystals*. Singapore: World Scientific.
- STEURER, W. (1989). *Acta Cryst.* **B45**, 534–542.

STEURER, W. (1991). *J. Phys. Condens. Matter*, **3**, 3397–3410.
 STEURER, W. & MAYER, J. (1989). *Acta Cryst.* **B45**, 355–359.

YAMAMOTO, A. & ISHIHARA, K. N. (1988). *Acta Cryst.* **A44**, 707–714.

Acta Cryst. (1992). **A48**, 901–906

The Joint Probability Distribution of Any Set of Phases Given Any Set of Diffraction Magnitudes. I. Theoretical Considerations

BY C. GIACOVAZZO

Istituto di Ricerca per lo Sviluppo di Metodologie Cristallografiche CNR, c/o Dipartimento Geomineralogico, Campus Universitario, 70124 Bari, Italy

M. C. BURLA

Dipartimento di Scienze della Terra, Università, 06100 Perugia, Italy

AND G. CASCARANO

Istituto di Ricerca per lo Sviluppo di Metodologie Cristallografiche CNR, c/o Dipartimento Geomineralogico, Campus Universitario, 70124 Bari, Italy

(Received 13 December 1992; accepted 6 May 1992)

Abstract

Conditional joint probability distribution functions $P(\varphi_1, \dots, \varphi_n | R_1, \dots, R_n, \dots, R_p)$ of any set of n phases given any set of p diffraction moduli are calculated. The distributions include terms up to order $1/N$ and involve both triplet and quartet contributions. Two types of formulae are derived, which may be considered as developments of two mathematical approaches described by Hauptman [*Acta Cryst.* (1975). **A31**, 680–687] and by Giacovazzo [*Acta Cryst.* (1975). **A31**, 252–259; *Acta Cryst.* (1976). **A32**, 91–99] for the estimation of the quartet invariants.

1. Introduction

The discovery (Hauptman & Karle, 1953) of the properties of the structure invariants and seminvariants has played a crucial role in the solution of the phase problem. Their estimation was the main-spring for the development of the joint probability distribution methods (Hauptman & Karle, 1953; Klug 1958). Such methods rely on the idea that certain combinations of phases (*i.e.* the structure invariants and seminvariants) can be estimated when the related structure factors have their observed values.

More recently, this point of view has been generalized by the neighbourhood principle (Hauptman, 1975, 1978) and by the representation method (Giacovazzo, 1977*a*, 1980*a*). Such contributions extended the range of application of direct methods; indeed, single n -phase structure invariants could be estimated *via* the overall prior information provided

by p moduli of structure factors, where p may be much larger than n . Asymptotically, p may coincide with the number of measured diffraction magnitudes. The standard technique is as follows.

(i) The joint probability distribution function

$$P(\varphi_1, \dots, \varphi_n, \dots, \varphi_p, R_1, \dots, R_p) \quad (1)$$

is first calculated.

(ii) The marginal distribution

$$P(\varphi_1, \dots, \varphi_n, R_1, \dots, R_n, \dots, R_p) \quad (2)$$

with $n < p$ is derived. Accordingly,

$$\begin{aligned} P(\varphi_1, \dots, \varphi_n, R_1, \dots, R_n, \dots, R_p) \\ = \int \dots \int P(\varphi_1, \dots, \varphi_n, \dots, \varphi_p, \\ R_1, \dots, R_n, \dots, R_p) d\varphi_{n+1} \dots d\varphi_p. \end{aligned}$$

(iii) The conditional distribution

$$P(\varphi_1, \dots, \varphi_n | R_1, \dots, R_p) \quad (3)$$

is derived, where $\varphi_1, \dots, \varphi_n$ are the phases that compose the n -phase structure invariant

$$\Phi = \varphi_1 + \varphi_2 + \dots + \varphi_n$$

that one wishes to estimate.

(iv) The conditional distribution

$$P(\Phi | R_1, \dots, R_p) \quad (4)$$

is obtained, which provides the desired estimate of Φ .

In this paper we will focus our attention on distributions (3) characterized by large values of n . The aim is not that of deriving estimates of single n -phase